Image Denoising via Group Sparsity Residual Constraint

Zhiyuan Zha[1, 3], Xin Liu[2], Ziheng Zhou[2], Xiaohua Huang[2], Jingang Shi[2],
Zhenhong Shang[3], Lan Tang[1], Yechao Bai[1], Qiong Wang[1], Xinggan Zhang[1,*]
1 School of Electronic Science and Engineering, Nanjing University, Nanjing 210023, China. 2. The Center for Machine Vision and Signal Analysis, University of Oulu, 90014, Finland. 3. School of Information Engineering and Automation, Kunming University of Science and Technology, Kunming 650500, China.

1. Motivation

Group sparsity or nonlocal image representation has shown great potential in image denoising. However, most of existing methods only consider the nonlocal self-similarity (NSS) prior of noisy input image, and thus the similar patches are collected only from degraded input, which makes the quality of image denoising largely depend on the input itself. In this paper we propose a new prior model for image denoising, called group sparsity residual constraint (GSRC). Different from the most existing NSS prior-based denoising methods, two kinds of NSS prior (i.e., NSS priors of noisy input image and pre-filtered image) are simultaneously used for image denoising. In particular, to boost the performance of group sparse-based image denoising, the concept of group sparsity residual is proposed, and thus the problem of image denoising is transformed into one that reduces the group sparsity residual. To reduce the residual, we first obtain a good estimation of the group sparse coefficients of the original image by pre-filtering and then the group sparse coefficients of noisy input image are used to approximate the estimation. To improve the accuracy of the nonlocal similar patches selection, an adaptive patch search scheme is proposed. Moreover, to fuse this two NSS priors better, an effective iterative shrinkage algorithm is developed to solve the proposed GSRC model. Experimental results have demonstrated that the proposed GSRC modeling outperforms many state-of-the-art denoising methods in terms of the objective and the perceptual qualities.

2. Group-based Sparse Representation

Similar to patch-based sparse representation, given a dictionary $\boldsymbol{D}_i$, which is often learned from each group, each group $\boldsymbol{X}_i$ can be sparsely represented as $\boldsymbol{B}_i = \boldsymbol{D}_i^T \boldsymbol{X}_i$ and solved by the following l_p norm minimization problem,

$$\boldsymbol{B}_i = \arg\min_{\boldsymbol{B}_i} \{ \| \boldsymbol{X}_i - \boldsymbol{D}_i^T \boldsymbol{B}_i \|_F^2 + \lambda_i \| \boldsymbol{B}_i \|_p \} \qquad (1)$$

In image denoising, the goal is to exploit group sparse-based model to recover $\boldsymbol{X}_i$ from noisy observation $\boldsymbol{Y}_i$ and solve the following minimization problem,

$$\boldsymbol{A}_i = \arg\min_{\boldsymbol{A}_i} \{ \| \boldsymbol{Y}_i - \boldsymbol{D}_i^T \boldsymbol{A}_i \|_F^2 + \lambda_i \| \boldsymbol{A}_i \|_p \} \qquad (2)$$

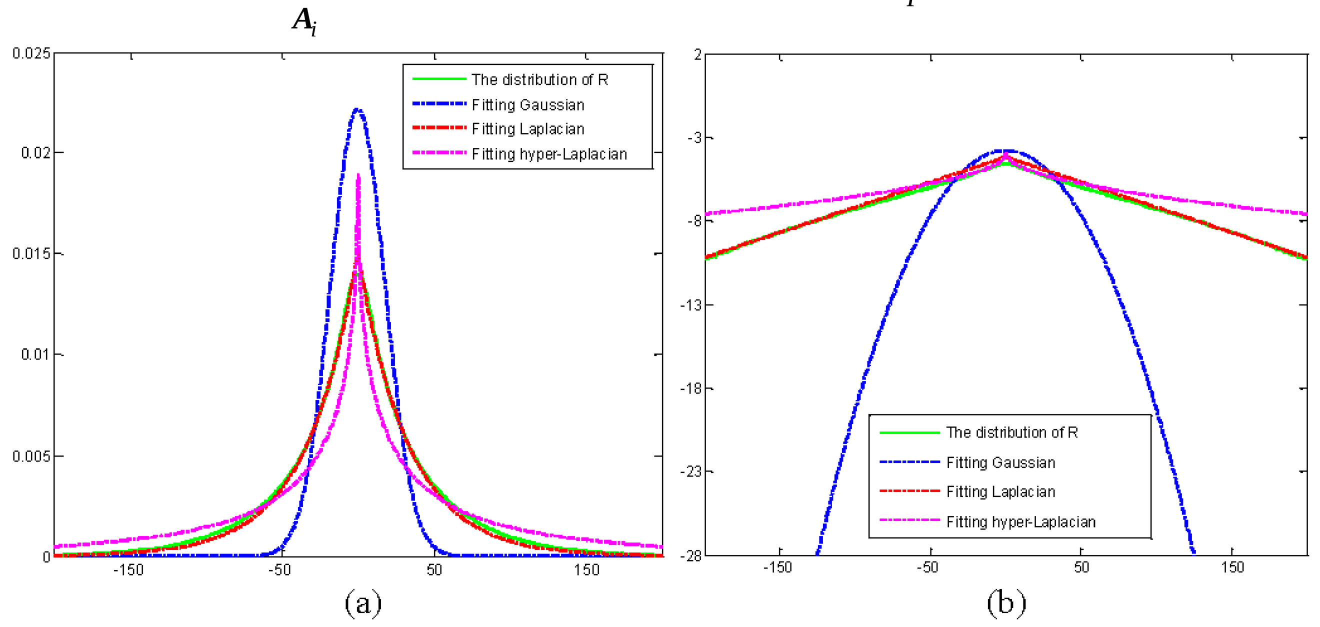

Fig2. The distribution of the group sparsity residual $\boldsymbol{R}$ for image *Parrots* with $\sigma = 50$ and fitting Gaussian, Laplacian and hyper-Laplacian distribution in (a) linear and (b) log domain, respectively (pre-filtering based on EPLL).

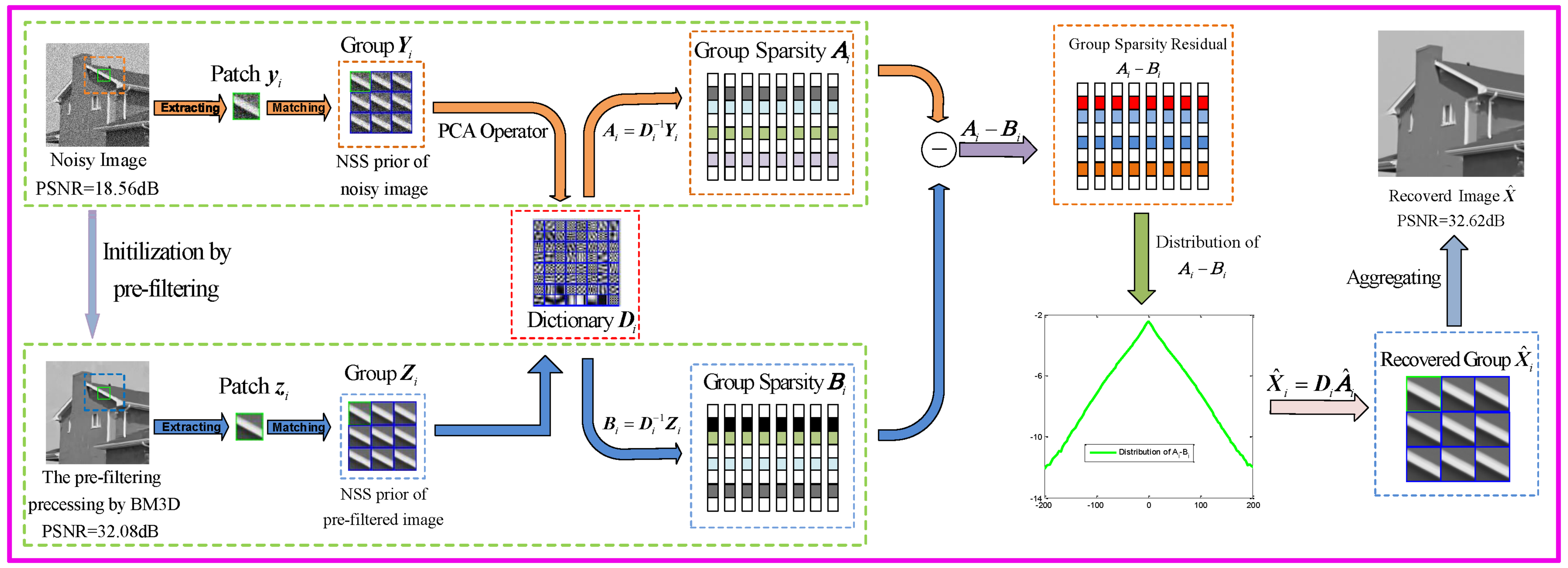

Fig1. Flowchart of image denoising by group sparsity residual constraint (GSRC) model

3. Group Sparsity Residual Constraint

Due to the influence of noise, it is very difficult to estimate the true group sparse code $\boldsymbol{B}$ from noisy image $\boldsymbol{Y}$. In other words, the group sparse code $\boldsymbol{A}$ obtained by solving (2) is expected to be close enough to the true group sparse code $\boldsymbol{B}$ of the original image $\boldsymbol{X}$. Thus, the quality of image denoising largely depends on the level of the group sparsity residual $\boldsymbol{R}$, we define

$$\boldsymbol{R} = \boldsymbol{A} - \boldsymbol{B} \qquad (3)$$

Thus, to reduce the group sparsity residual $\boldsymbol{R}$ and boost the accuracy of $\boldsymbol{A}$, we propose a new prior model to image denoising, called group sparse residual constraint (GSRC), and thus (2) can be rewritten as

$$\boldsymbol{A}_i = \arg\min_{\boldsymbol{A}_i} \{ \| \boldsymbol{Y}_i - \boldsymbol{D}_i^T \boldsymbol{A}_i \|_F^2 + \lambda_i \| \boldsymbol{A}_i - \boldsymbol{B}_i \|_p \} \qquad (4)$$

4. Iterative Shrinkage Algorithm

For fixed $\boldsymbol{B}_i$ and λ_i, we adopt an iterative shrinkage algorithm to solve Eq. (4). In the *t*-iteration, the proposed shrinkage operator can be calculated as

$$\hat{\boldsymbol{A}}_i^{t+1} = \boldsymbol{S}_{\lambda_i}(\boldsymbol{D}_i^T \boldsymbol{X}_i^t - \boldsymbol{B}_i) + \boldsymbol{B}_i \qquad (5)$$

5. Adaptive patch search

*k*NN method has been widely used to nonlocal similar patch selection. However, since the given reference patch is noisy, *k*NN has a drawback that some of the *k* selected patches may not be truly similar to given reference patch. Thus, in order for an effective similar patches indexes by *k*NN, an adaptive patch search scheme is proposed, i.e.,

$$\partial = \mathrm{SSIM}(\boldsymbol{Z}, \boldsymbol{X}^{t+1}) - \mathrm{SSIM}(\boldsymbol{Z}, \boldsymbol{X}^t) \qquad (6)$$

where SSIM represents structural similarity, X^t represents the *t*-th iteration denoising result. We empirically define that if $\partial < \tau$, then the reconstructed image X^{t+1} is regarded as target image to fetch the *k* similar patches, otherwise the pre-filtered image $\boldsymbol{Z}$ is regarded as target image, such as BM3D and EPLL.

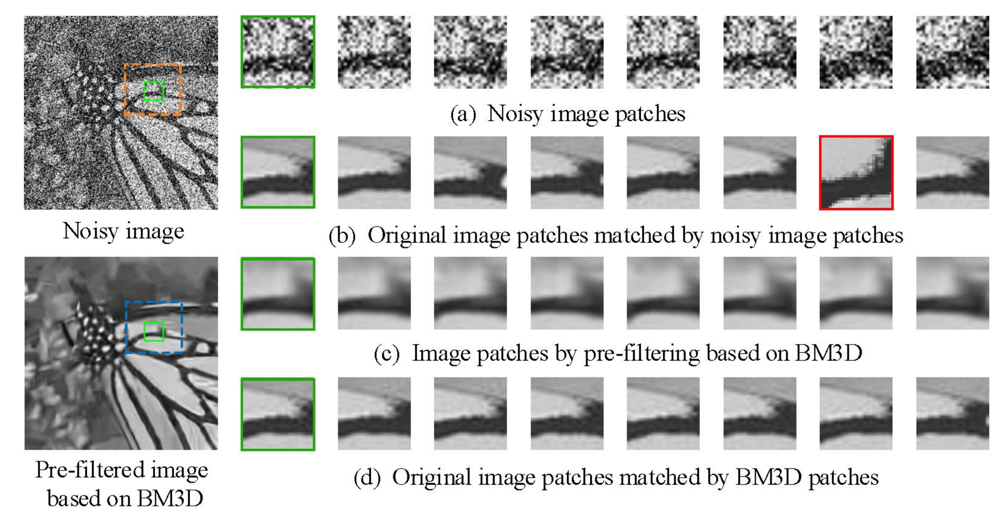

Fig.3 Patch selection between noisy image and pre-filtered image based on BM3D via *k*NN method (where green box represents the reference patch).

σ	20	30	40	50	75	100
NCSR	29.89	27.92	26.58	25.65	24.04	23.00
GID	28.87	27.00	25.87	24.97	23.37	22.20
LINC	29.95	27.98	26.68	25.73	24.11	23.02
MS-EPLL	29.95	28.02	26.73	25.84	24.29	23.27
AST-NLS	29.98	28.02	26.68	25.80	24.20	23.17
WNNM	30.11	28.17	26.88	25.96	24.42	23.37
GSRC-BM3D	**30.13**	**28.18**	**26.89**	**25.98**	**24.45**	**23.40**
GSRC-EPLL	**30.91**	**28.85**	**27.48**	**26.45**	**24.74**	**23.62**

Table1 Average PSNR (dB) results of different denoising algorithms for Gaussian denoising with noise level 20, 30, 40, 50, 75 and 100 on BSD200 dataset.

σ	20	30	40	50	75	100
NCSR	213.97	214.74	469.84	466.78	349.50	348.35
GID	345.92	345.84	345.71	345.74	346.05	345.86
LINC	261.94	256.99	251.42	252.21	247.21	253.33
MS-EPLL	222.66	147.09	147.00	210.63	210.74	210.69
AST-NLS	184.27	279.79	280.27	451.41	641.93	846.11
WNNM	100.92	211.35	212.14	163.30	261.69	262.23
GSRC-BM3D	**31.47**	**65.08**	**60.20**	**62.70**	**84.27**	**139.61**
GSRC-EPLL	117.00	162.77	165.23	166.94	**139.76**	213.48

Table2 Average run time (s) with different standard deviation of NCSR, GID, LINC, MS-EPLL, AST-NLS, WNNM, GSRC-BM3D and GSRC-EPLL methods on the 16 test images (size: 256 × 256).

σ	15	25	50	75
MLP	-	29.09	26.05	24.55
TNRD	31.65	29.08	26.02	-
Dn-CNN	32.01	29.43	26.32	24.65
GSRC-BM3D	31.61	29.02	25.98	24.45
GSRC-EPLL	**32.41**	**29.75**	**26.45**	**24.74**

Table 3 Average PSNR (dB) results of different denoising algorithms for Gaussian denoising with noise level 15, 25, 50 and 50 on BSD200 dataset .

6. Performance Comparison with the State-of-the-Art Methods

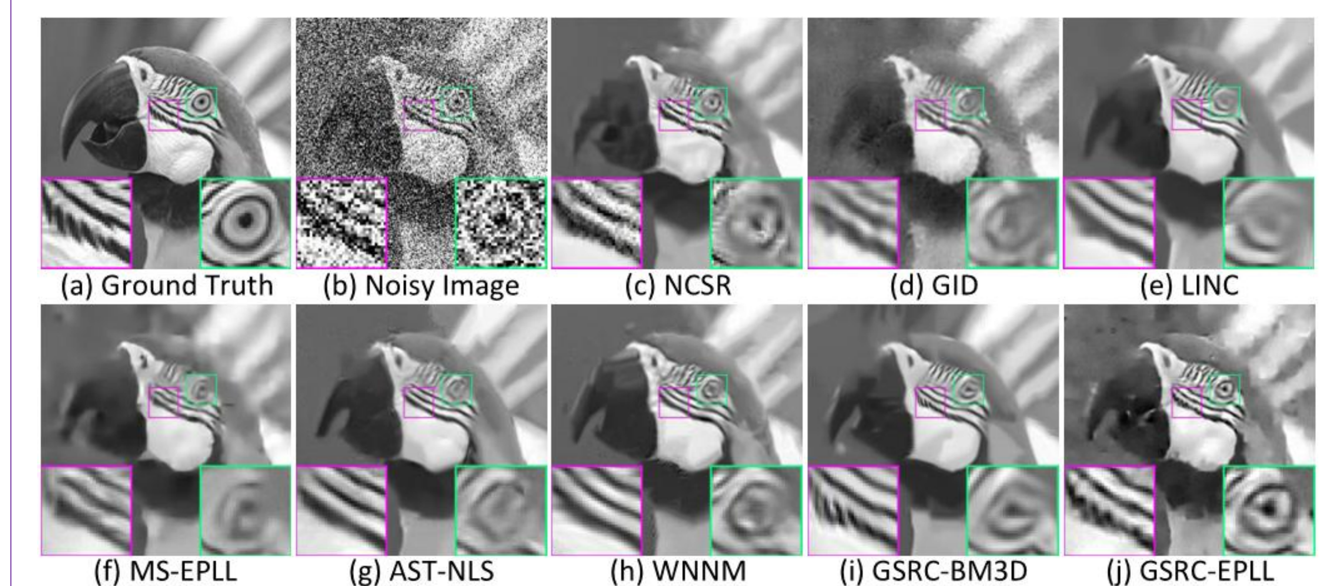

Fig.4 Denoising images of *Parrot* by different methods ($\sigma = 100$). (a) Ground Truth; (b) Noisy image; (c) NCSR (PSNR= 24.36dB); (d) (PSNR= 23.54dB); (e) LINC (PSNR= 24.46dB); (f) MS-EPLL (PSNR= 24.38dB); (g) AST-NLS (PSNR= 24.81dB); (h) WNNM (PSNR= 24.94dB); (i) GSRC-BM3D (PSNR= **25.17dB**); (j) GSRC-EPLL (PSNR = **25.14dB**).

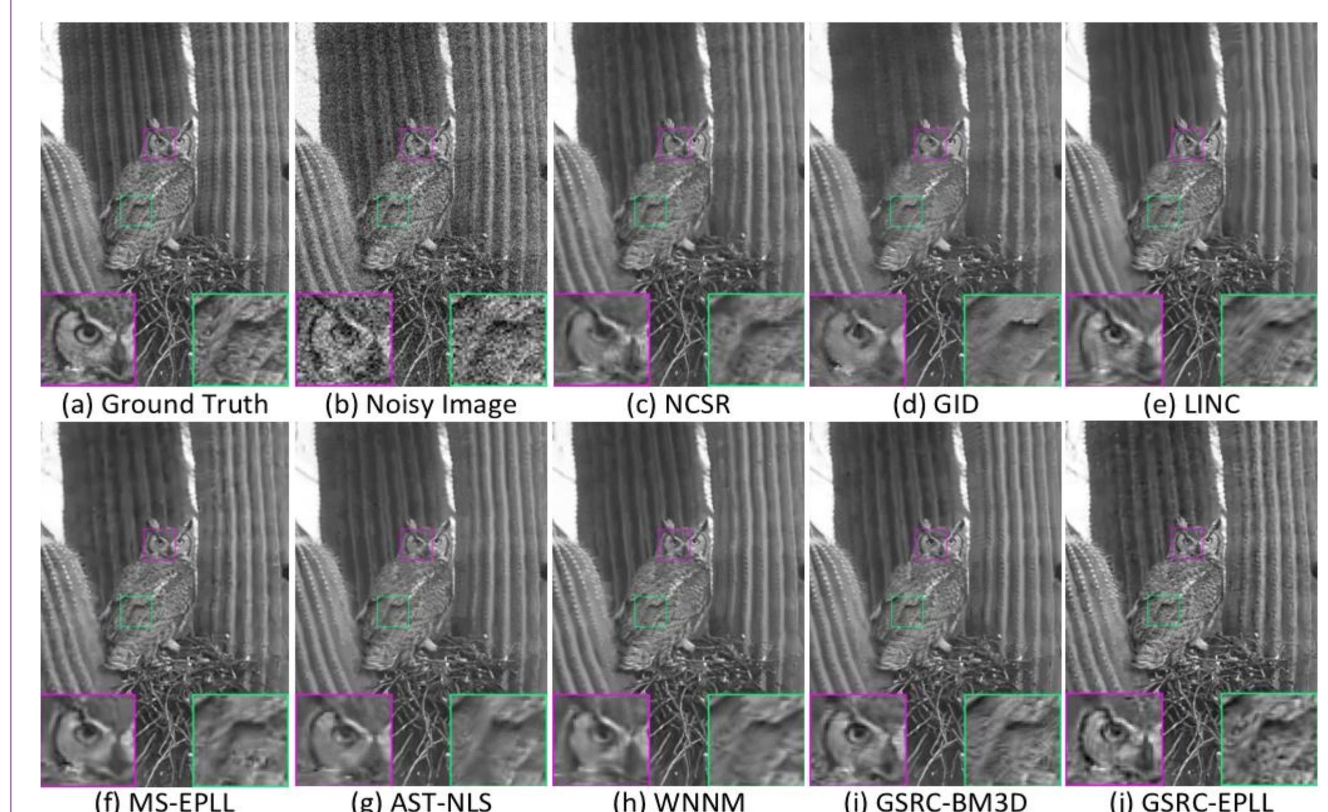

Fig. 5 Denoising images of *196040* by different methods ($\sigma = 30$). (a) Ground Truth; (b) Noisy image; (c) NCSR (PSNR= 25.83dB); (d) GID (PSNR= 24.89dB); (e) LINC (PSNR= 25.96dB); (f) MS-EPLL (PSNR= 25.90dB); (g) AST-NLS (PSNR= 26.06dB); (h)WNNM (PSNR= 26.04dB); (i) GSRC-BM3D (PSNR= **26.16dB**); (j) GSRC-EPLL (PSNR =**26.86dB**).

7. Performance Comparison with the Deep Learning based Methods

Fig.6 Denoising images of *15011* by different methods ($\sigma = 25$). (a) Ground Truth; (b) Noisy image; (c) MLP (PSNR= 29.32dB); (d) TNRD (PSNR= 29.26dB); (e) Dn-CNN (PSNR= 29.46dB); (f) GSRC-EPLL (PSNR= **30.01dB**).

Reference

[1] Dong W, Zhang L, Shi G, et al. Nonlocally centralized sparse representation for image restoration, TIP 2013.
[2] Talebi H, Milanfar P. Global image denoising, TIP 2014.
[3] Niknejad M, Rabbani H, Babaie-Zadeh M. Image restoration using Gaussian mixture models with spatially constrained patch clustering, TIP2015.
[4] Papyan V, Elad M. Multi-scale patch-based image restoration, TIP 2016.
[5] Liu H, Xiong R, Zhang J, et al. Image denoising via adaptive soft-thresholding based on non-local samples, CVPR2015.
[6] Gu S, Zhang L, Zuo W, et al. Weighted nuclear norm minimization with application to image denoising, CVPR2014.
[7] Burger H C, Schuler C J, Harmeling S. Image denoising: Can plain neural networks compete with BM3D? , CVPR2012.
[8] Chen Y, Pock T. Trainable nonlinear reaction diffusion: A flexible framework for fast and effective image restoration, PAMI 2016.
[9] Beyonda gaussian denoiser: Residual learning of deep cnn for image denoising, TIP2017.
[10] Dabov K, Foi A, Katkovnik V, et al. Image denoising by sparse 3-D transform-domain collaborative filtering, TIP 2007.
[11] Zoran D, Weiss Y. From learning models of natural image patches to whole image restoration, ICCV 2011.